Proceedings of the Canadian Society for Mechanical Engineering International Congress
32nd Annual Conference of the Computational Fluid Dynamics Society of Canada
Canadian Society of Rheology Symposium

CSME/CFDSC/CSR 2025

Fluid Viscosity Effects on Carbon Anode Vibro-compaction

Amir Kafaei[1,2], Louis Gosselin[2,3], Houshang Darvishi Alamdari[2,4], Seyed Mohammad Taghavi[1,2*]

[1]Department of Chemical Engineering, Université Laval, Québec, Canada
[2]Aluminium Research Center (REGAL), Québec, Canada
[3]Department of Mechanical Engineering, Université Laval, Québec, Canada
[4]Department of Mining, Metallurgical, and Materials Engineering, Université Laval, Québec, Canada
[*]Seyed-Mohammad.Taghavi@gch.ulaval.ca

***Abstract*—**Carbon anodes, commonly made by vibro-compaction of anode paste, are an important part of the electrolytic reaction in aluminum production. The overall behavior of anode paste during vibro-compaction is greatly influenced by the properties of coke aggregates and the rheological characteristics of pitch, particularly its viscosity. To simulate this process and investigate the effect of fluid viscosity, we use mixtures of coke particles (80% by volume) combined with a fluid (20% by volume) consisting of glycerin and water. The glycerin-to-fluid volume fraction is varied across four ratios: 70%, 80%, 90%, and 100%. The reason for using a mixture of glycerin and water as a representative fluid is that its viscosity at room temperature resembles the viscosity of the binder matrix (a mixture of coal tar pitch and fine coke particles) at high temperatures in the vibra-compaction stage, as determined through dimensional analysis. Using ultra-high-speed imaging at 3,000 frames per second, we track the representative materials' dynamics when poured into a transparent vessel and subjected to vertical vibration at 60 Hz frequency and 0.4 mm amplitude. Then, we analyze the effect of glycerine-to-water volume fraction on the bulk average height and height uniformity. Our results show that the vibration activates the void-filling mechanism, minimizes the voids between the particles, and compacts the bulk material through time. In addition, the compaction rate and final degree of uniformity are affected by the glycerin-to-fluid volume fraction. Specifically, mixtures with a lower glycerin-to-fluid volume fraction, indicating a lower viscosity, showed faster compaction and achieved a more uniform final surface profile. The reason is that the lower viscosity of water compared to glycerin reduces interparticle forces and facilitates particle rearrangement during vibration. Our findings contribute to a deeper understanding of vibro-compaction and have potential implications for various vibration-based industrial processes, including those in the pharmaceutical, food processing, and sediment transport. Furthermore, the experimental setup and image analysis techniques developed in this study can be used to investigate the effect of other parameters, such as particle size and vibration frequency, on the vibration-induced dynamics of granular materials.

***Keywords-component*—Aluminum production, Carbon anodes, Granular materials, Vibration, Compaction**

I. INTRODUCTION

Granular materials are widely used in engineering and exhibit complex behavior when subjected to vibration. Understanding this complexity is crucial for both natural processes, such as landslides and earthquakes, and industrial applications, such as vibro-compaction of anode paste in carbon anode production [1–3]. Carbon anodes are key components in the electrolysis reaction that converts alumina to molten aluminum. Since carbon anodes are consumed during this reaction, their density and homogeneity significantly impact the overall performance of aluminum production [4]. Figure 1 shows sequential stages of anode production: preparation of raw materials (coal-tar pitch and calcined petroleum coke particles), mixing, vibro-compaction of anode paste, and the final baked carbon anode [5].

Green anodes are made by vibro-compacting anode paste in a mold [6]. The vibro-compaction chamber is first filled with a mixture of calcined petroleum coke particles and coal-tar pitch, forming a semi-conical heap. Research shows that porosity is lowest in the core of the bulk material and increases in a V-shaped distribution towards the edges [7]. This porosity distribution indicates that the core area is more compacted than the sides, even before further compaction occurs from the descending flat plate. Additionally, the pouring process causes significant horizontal size segregation in the bulk material: coarse particles, due to their higher inertia, tend to accumulate in the outer area, while smaller particles remain concentrated in the interior section [8].

One key characteristic of a poured granular material is the angle of repose (AoR), defined as the steepest angle at which a bulk can be placed without slumping relative to the horizontal plane [9]. The angle of repose is a key property that characterizes the cohesive behavior of granular materials. It also effectively indicates the material's filling capacity, packing stability, and behavior under various conditions, particularly when subjected to vibration [10].

Particle diameter is one of the parameters that affects the angle of repose; nevertheless, the nature of this influence is not invariably straightforward. Some studies have found that

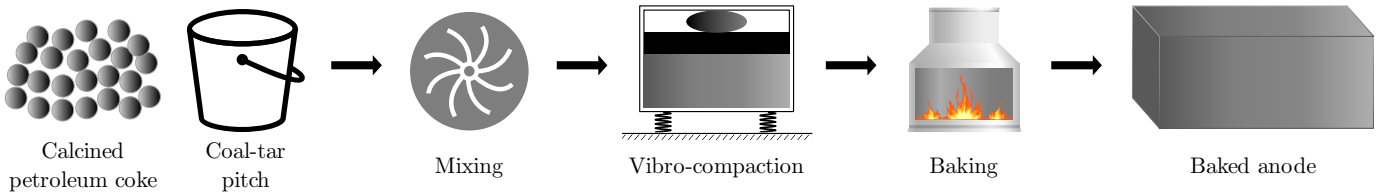

Figure. 1. Step-by-step process for manufacturing carbon anodes. The procedure involves initial preparation of coal-tar pitch and calcined petroleum coke, followed by mixing, vibro-compaction, and ultimately baking to produce the final product.

large particles exhibit greater interlocking and resistance to slippage and rolling due to their increased surface area and more friction, leading to a higher angle of repose [11–14]. In contrast, the findings of other studies suggest that smaller particles tend to form a bulk with a higher angle of repose due to higher surface area to volume ratio, more contact points, and stronger interparticle forces [8, 15]. In addition to the particle size, other particle properties also affect the flowability of a material. Static and rolling friction coefficients, influenced by particle texture, significantly affect repose angle most among all considered parameters [16]. Research indicates that a higher friction coefficient increases the angle of repose, which in turn results in a decrease in flowability [8]. In addition, irregularly shaped particles form a bulk with a higher angle of repose, which is explained by the enhanced interlocking between the irregular aggregates [10].

The interplay between the lubricating effects of a liquid and cohesive forces promoted by its viscosity affects flowability of wet granular materials. On the one hand, higher water content reduces interparticle friction, allowing the particles to flow more easily [12, 17–20]. On the other hand, water can increase capillary forces and cohesion between particles, leading to clumping, poorer flow characteristics, and higher angle of repose [21–25]. It is found that a more viscous fluid exerts a greater drag force. Increased drag force stabilizes granular flow, decreases particle collisions, slows relative motion, and decreases velocity fluctuations. In addition, it leads to the forming of a more stable pile with stronger cohesive forces, lower segregation, higher angles of repose, and stronger liquid bridges [21, 26, 27]. Since particles are less likely to segregate in a cohesive environment, the final segregation index decreases as viscosity increases [21]. Moreover, higher cohesivity promotes clumping and reduces flowability, affecting the angle of repose and fluidization behavior.

After pouring the material into the vibro-compaction chamber, a flat plate descends on the bulk material, applying pressure while vibrating vertically. The stress caused by the load begins to move from the top layers to the entire bulk, while the vibration allows coke particles to flow from the pile center to the sides, resulting in a more uniform distribution. Fluidization is one of the common phenomena observed in vibrated granular materials, in which the material transits from a solid-like to a fluid-like state [28]. This transition is mainly caused by the weakened inter-particle friction, enabling the particles to flow more freely. The fluidization dynamics are affected by vibration frequency, amplitude, particle properties, and fluid characteristics [29].

Segregation is another phenomenon that occurs in polydisperse granular materials when subjected to vertical vibration. This phenomenon is known as the Brazil nut effect, where larger aggregates tend to rise to the bulk surface while smaller ones accumulate at lower layers [30]. It is shown that the size and density of particles, in addition to the rheological characteristics of the fluid, play a significant role in the segregation of the granular material under vibration [31].

While considerable research has been conducted on the vibration-induced dynamics of granular materials, further investigation is required to understand the time-dependent variations in bulk average height and uniformity. Additionally, it is crucial to explore how fluid viscosity, particularly glycerin and water volume fractions, influences the temporal evolution of bulk material during vibration. We, therefore, analyzed the effect of glycerin-water volume fraction on several parameters, including the variation of bulk angle over time and the changes in bulk uniformity throughout the vibration period.

To begin our analysis, we first outline the experimental setup for pouring and inducing vibration to granular materials. Next, we present the time-dependent changes in bulk surface curvature observed during vertical vibration. Following this, we compare the average height and height uniformity across different glycerin and water volume fractions. Finally, we summarize the key findings from our experiments and discuss potential avenues for future research in this area.

II. Materials and Methods

This section describes the experimental setup, experimental procedure, and image processing methods.

A. *Experimental setup*

Our lab-scale experimental setup, shown in Figure 2, is designed to simulate the industrial vibro-compaction. The setup consists of a $10 \times 10 \times 2$ cm^3 transparent vessel [32]. These dimensions ensure that the side walls have minimum effect on the bulk dynamics during pouring and vibration [33]. The vessel is installed firmly on a “Vibro Pro Kinetic” vibration table, which provides vertical vibrations at a frequency of 60 Hz and an amplitude of 0.4 mm. To capture the dynamics of the granular materials at 3,000 frames per second, a “FASTCAM SA-Z” ultra-high-speed camera is used. We use LED-lit lightboxes and diffusive panels to enhance lighting conditions to achieve high-quality images at these

high frame rates. All experiments are conducted at a controlled temperature of 20 ± 0.5 °C to ensure reproducibility.

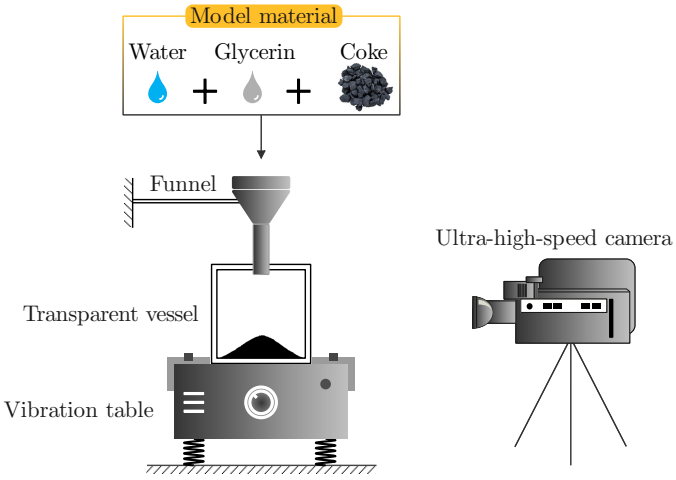

Figure. 2. Schematic illustration of the granular flow apparatus. A transparent container mounted on a vibrating platform enables the observation of bulk motion, with material introduced through a funnel and dynamics captured via ultra-high-speed imaging.

B. Experimental procedure

To prepare the material, specific volumes of coke particles, glycerin, and distilled water are thoroughly mixed. The mixture is then poured into a vessel, forming a semi-conical heap. Next, the bulk is subjected to a two-second vertical vibration with 60 Hz frequency and 0.4 mm amplitude. Meanwhile, an ultra-high-speed camera captures 3,000 frames per second. Given the 60 Hz frequency of the vibration table, 50 images will be obtained for each oscillation of the vibration table.

C. Image processing

After conducting the experiments, a MATLAB code is used to track and monitor the bulk motion and vibration table displacement [32]. First, the captured images are cropped to a specific preset region. For each x-coordinate, the code stores the first y-coordinate of the pixel that exceeds a defined brightness threshold, indicating the bulk surface profile in each image. The bulk average height is calculated as the mean of the y-coordinates of the surface profile across all x-coordinates:

$$\hat{\bar{z}}_B = \frac{1}{N_x} \sum_{x=1}^{N_x} \hat{z}(x) \tag{1}$$

where $\hat{z}(x)$ is the height of the surface at each x-coordinate, and N_x is the total number of x-coordinates.

We also define height uniformity, a dimensionless parameter quantifying the evenness of the surface profile, as follows:

$$u_B = 1 - \frac{\sigma_z}{\hat{z}_{\max} - \hat{z}_{\min}} \tag{2}$$

where σ_z is the standard deviation of the y-coordinates of the surface profile, and $\hat{z}_{\max}$ and $\hat{z}_{\min}$ are the maximum and minimum y-coordinates of the surface profile, respectively.

III. Results and Discussions

First, it is essential to define two key parameters: the particle volume fraction (ϕ) and the glycerin-to-fluid volume fraction (ζ).

The particle volume fraction (ϕ) is defined as the ratio of the volume of coke particles ($\hat{V}_c$) to the total volume of the mixture, which includes the volumes of coke ($\hat{V}_c$), glycerin ($\hat{V}_g$), and water ($\hat{V}_w$):

$$\phi = \frac{\hat{V}_c}{\hat{V}_c + \hat{V}_g + \hat{V}_w} \tag{3}$$

In all the cases considered in this study, the particle volume fraction is kept constant at 80%, similar to the anode paste recipe in vibro-compaction.

The glycerin-to-fluid volume fraction (ζ) is defined as the ratio of the volume of glycerin ($\hat{V}_g$) to the total volume of the fluid, which includes the volumes of glycerin ($\hat{V}_g$) and water ($\hat{V}_w$):

$$\zeta = \frac{\hat{V}_g}{\hat{V}_g + \hat{V}_w} \tag{4}$$

We aim to analyze the dynamics of granular materials during vibro-compaction. Figure 3 shows how a granular bulk (with $\phi = 80\%$ and $\zeta = 70\%$) evolutes over time during vertical vibration. The 2D bulk surface profiles are displayed at a series of intervals (0.0 s, 0.5 s, 1.0 s, 1.5 s, and 2.0 s). Darker blue shades indicate earlier times, while lighter blue shades show later stages.

Initially ($t = 0.0$ s), the granular material forms a cone-shaped heap with a steep surface slope (angle of repose), indicating that the particles are packed loosely right after being poured. This loose configuration is characterized by a significant presence of void spaces between the particles, resulting in a lower overall bulk density.

After initiating the vibration, the material begins to compact dynamically, with particles redistributing over time. This phase is characterized by reduced bulk average height and angle. The initial height of the bulk decreases continuously over time as particles settle and fill void spaces. Vibration facilitates particle motion, causing them to flow downward and find more stable configurations. This compaction effect is particularly pronounced in the central region of the bulk. In addition, the bulk angle decreases due to the combined effects of particle rearrangement and reduced void space. As the angle of repose decreases, the material becomes more stable and has less tendency to slump. The reduced angle also indicates improved uniformity in particle distribution across the bulk.

By the end of the vibration period ($t = 2.0$ s), the bulk surface stabilizes, reaching a nearly uniform height and angle, though the average height continues to decrease slightly. The resulting profile is flatter compared to the initial state, indicating a reduction in the angle of repose. The final angle represents the most stable configuration under the applied vibration. In addition, this state represents the maximum achievable compaction with minimal void spaces under the

given vibration conditions (frequency of 60 Hz and amplitude of 0.4 mm).

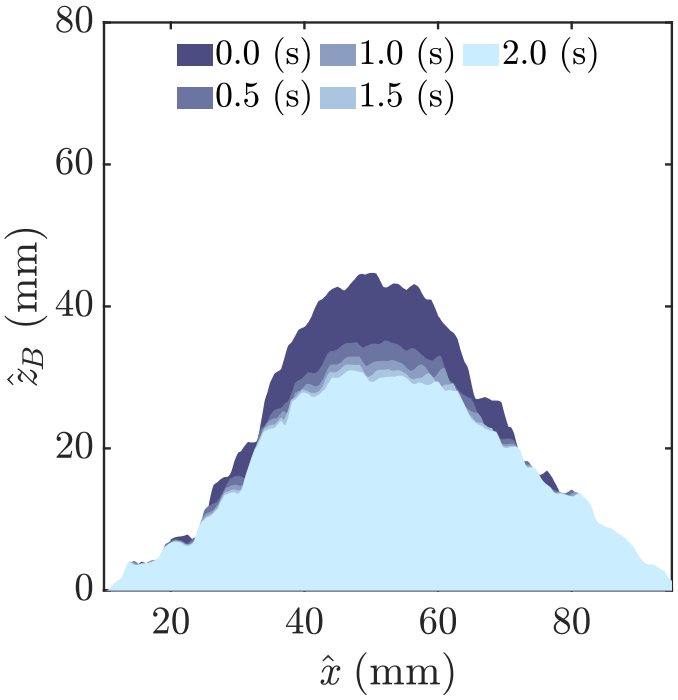

Figure. 3. Dynamic bulk compaction under vibration for a granular material with $\phi = 80\%$ and $\zeta = 70\%$. The 2D bulk evolution is visualized from the initial state ($\hat{t} = 0.0$ s) to the final state ($\hat{t} = 2.0$ s). Darker blue shades represent earlier times, while lighter blue shades indicate later times, with profiles shown at intervals of 0.5 s.

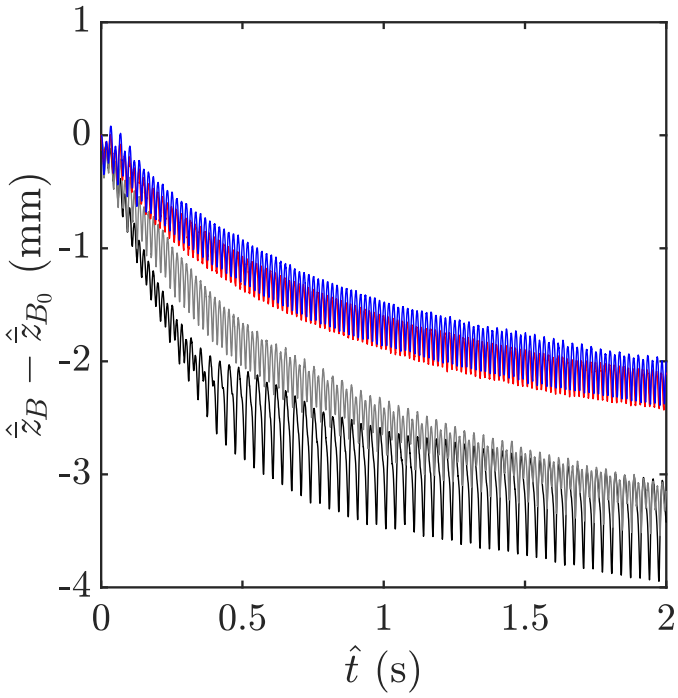

Figure. 4. Time evolution of the bulk average height ($\hat{\bar{z}}_B$) for different glycerin-to-fluid volume fractions (ζ). The bulk average height is normalized by subtracting the initial height ($\hat{\bar{z}}_{B_0}$) for each case. The particle volume fraction (ϕ) is kept constant at 80%. The black, gray, blue, and red lines represent ζ values of 70%, 80%, 90%, and 100%, respectively. The decrease in bulk average height over time indicates the compaction of the granular material under vertical vibration. The presence of water in the fluid mixture (lower ζ values) enhances the compaction process, as evidenced by the faster decrease in bulk average height.

In this study, four cases are compared with varying glycerin to fluid volume fractions: 70% (black line in Figure 4 and Figure 5), 80% (gray line), 90% (blue line), and 100% (red line, representing the case with only glycerin as the fluid).

Figure 4 illustrates the time evolution of the bulk average height ($\hat{\bar{z}}_B$) for the four cases with different glycerin-to-fluid volume fractions. The figure shows that the bulk average height decreases with time for all four cases, indicating the compaction of the granular material under vertical vibration. The case with the highest glycerin to fluid volume fraction (100%, red line) exhibits the slowest decrease in bulk average height, while the case with the lowest glycerin to fluid volume fraction (70%, black line) shows the fastest decrease. Furthermore, the range at which the average height oscillates is wider for cases with higher water and lower glycerin content. This observation suggests that the presence of water in the fluid mixture enhances the compaction process, likely due to the lower viscosity of water compared to glycerin.

Figure 5 presents the time evolution of the height uniformity (u_B) for the four cases. The figure shows that the height uniformity increases with time for all four cases, indicating that the surface profile becomes more even as the granular material compacts under vertical vibration. The case with the highest glycerin-to-fluid volume fraction (100%, red line) exhibits the slowest increase in height uniformity, while the case with the lowest glycerin-to-fluid volume fraction (70%, black line) shows the fastest increase. This observation suggests that the presence of water in the fluid mixture promotes the formation of a more uniform surface profile during the compaction process.

IV. Conclusion

This study experimentally examined the dynamics of granular materials subjected to vertical vibration. Mixtures of coke particles, glycerin, and water were used to simulate the anode paste in the vibro-compaction process. Vertical vibration was then applied to the poured material, while ultra-high-speed imaging captured the bulk motion and vibration table displacement at 3,000 frames per second.

The results demonstrated the influence of the glycerin-to-fluid volume fraction on the compaction dynamics of the granular material under vertical vibration. A lower glycerin-to-fluid volume fraction, indicating a lower overall viscosity of the fluid, enhanced the compaction process and promoted the formation of a more uniform surface profile, likely due to the lower viscosity of water compared to glycerin. In addition, the range at which the average height oscillated was wider for cases with higher water and lower glycerin content. These findings provided valuable insights into the role of fluid properties in the vibro-compaction process and can guide the

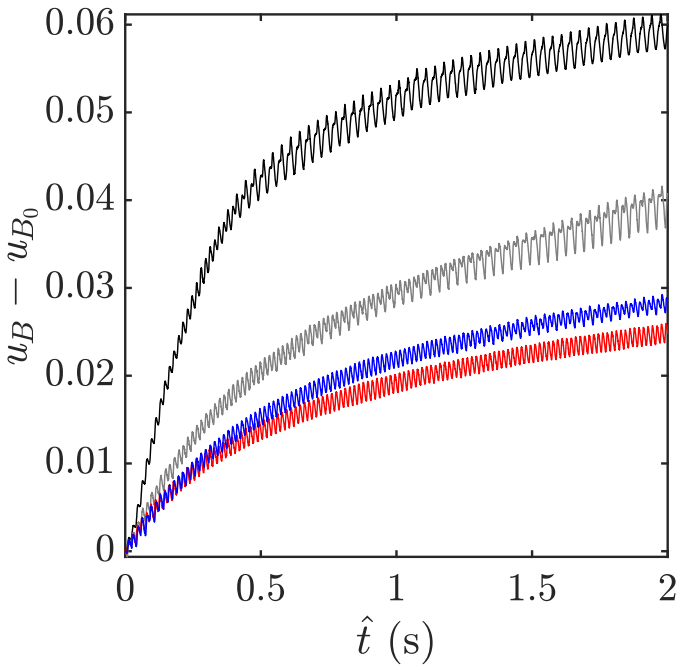

Figure. 5. Time evolution of the height uniformity (u_B) for different glycerin-to-fluid volume fractions (ζ). The height uniformity is normalized by subtracting the initial height uniformity (u_{B_0}) for each case. The particle volume fraction (ϕ) is kept constant at 80%. The black, gray, blue, and red lines represent ζ values of 70%, 80%, 90%, and 100%, respectively. The increase in height uniformity over time indicates that the surface profile becomes more even as the granular material compacts under vertical vibration. The presence of water in the fluid mixture (lower ζ values) promotes the formation of a more uniform surface profile during the compaction process, as evidenced by the faster increase in height uniformity.

optimization of industrial applications, such as the production of carbon anodes for aluminum smelting.

Acknowledgments

This research has been conducted at Université Laval. We gratefully acknowledge financial support from Alcoa Corporation and the Natural Sciences and Engineering Research Council of Canada (NSERC) through an Alliance grant. Additional support was provided by the Canada Foundation for Innovation (CFI) under Grant Nos. GF130120, GQ130119, and GF525075, the Canada Research Chairs Program for the Modeling of Complex Flows (Grant No. CG125810), the NSERC Research Tools and Instruments Grant (Grant No. CG132931), and the NSERC Discovery Grant (Grant No. CG109154).

References

[1] M. Sun, R. Mollaabbasi, B. Li, H. Alamdari, M. Fafard, and S.M. Taghavi. Single and multiscale bubble motions beneath an inclined downward-facing surface in the aluminum reduction cell. *Industrial and Engineering Chemistry Research*, 59(17):8403–8415, 2020.

[2] M. Madrid, J. Fuentes, F. Ayuga, and E. Gallego. Determination of the angle of repose and coefficient of rolling friction for wood pellets. *Agronomy*, 12(2):424, 2022.

[3] W. Niu, H. Zheng, W. Mao, and Y. Huang. Effects of vibration on granular chute flow under low-gravity conditions. *Powder Technology*, 438:119604, 2024.

[4] Q. Wang, L. Gosselin, M. Fafard, J. Peng, and B. Li. Numerical investigation on the impact of anode change on heat transfer and fluid flow in aluminum smelting cells. *Metallurgical and Materials Transactions B*, 47:1228–1236, 2016.

[5] R. Mollaabbasi, L. Hansen, T. Grande, S.M. Taghavi, and H. Alamdari. Effect of fine coke particles on rheological properties of the binder matrix of carbon anodes in alumi m production process. *The Canadian Journal of Chemical Engineering*, 100:58–71, 2022.

[6] B. Chen, H. Chaouki, D. Picard, J. Lauzon-Gauthier, H. Alamdari, and M. Fafard. Modeling of thermo-chemo-mechanical properties of anode mixture during the baking process. *Materials*, 14(15):4320, 2021.

[7] H. Wei, X. Tang, Y. Ge, M. Li, H. Saxén, and Y. Yu. Numerical and experimental studies of the effect of iron ore particle shape on repose angle and porosity of a heap. *Powder Technology*, 353:526–534, 2019.

[8] C. Li, T. Honeyands, D. O'Dea, and R. Moreno-Atanasio. The angle of repose and size segregation of iron ore granules: DEM analysis and experimental investigation. *Powder Technology*, 320:257–272, 2017.

[9] A. Taghizadeh, S. Hashemabadi, E. Yazdani, and S. Akbari. Numerical analysis of restitution coefficient, rotational speed and particle size effects on the hydrodynamics of particles in a rotating drum. *Granular Matter*, 20:1–13, 2018.

[10] B. Dai, J. Yang, and C. Zhou. Micromechanical origin of angle of repose in granular materials. *Granular Matter*, 19(2):24, 2017.

[11] D. Höhner, S. Wirtz, and V. Scherer. A study on the influence of particle shape and shape approximation on particle mechanics in a rotating drum using the discrete element method. *Powder Technology*, 253:256–265, 2014.

[12] N. Cheng and K. Zhao. Difference between static and dynamic angle of repose of uniform sediment grains. *International Journal of Sediment Research*, 32(2):149–154, 2017.

[13] T. Roessler and A. Katterfeld. Scaling of the angle of repose test and its influence on the calibration of DEM parameters using upscaled particles. *Powder Technology*, 330:58–66, 2018.

[14] A. Hamed, Y. Xia, N. Saha, J. Klinger, D. Lanning, and J. Dooley. Flowability of crumbler rotary shear size-reduced granular biomass: An experiment-informed modeling study on the angle of repose. *Frontiers in Energy Research*, 10:859248, 2022.

[15] H. Nakashima, Y. Shioji, T. Kobayashi, S. Aoki, H. Shimizu, J. Miyasaka, and K. Ohdoi. Determining the angle of repose of sand under low-gravity conditions using discrete element method. *Journal of Terramechanics*, 48(1):17–26, 2011.

[16] R. Cunha, K.G. Santos, R.N. Lima, C.R. Duarte, and M.A.S. Barrozo. Repose angle of monoparticles and binary mixture: An experimental and simulation study. *Powder Technology*, 303:203–211, 2016.

[17] A. Szalay, A. Kelemen, and K. Pintye-Hódi. The influence of the cohesion coefficient (c) on the flowability of different sorbitol types. *Chemical Engineering Research and Design*, 93:349–354, 2015.

[18] R. Bhadra, M. Casada, S. Thompson, J. Boac, R. Maghirang, M. Montross, A. Turner, and S. McNeill. Field-observed angles of repose for stored grain in the United States. *Applied Engineering in Agriculture*, 33(1):131–137, 2017.

[19] M. Zhang, G. Yu, W. Zhu, and M. Li. Experimental study on the angle of repose of submerged cohesive sediments. *Journal of Waterway, Port, Coastal, and Ocean Engineering*, 145(3):04019006, 2019.

[20] H. Kalman and D. Portnikov. Underwater measurements of flowability by angle of repose, Hausner ratio and Jenike shear cell. *Powder Technology*, 429:118883, 2023.

[21] S. Chou, C. Liao, and S. Hsiau. An experimental study on the effect of liquid content and viscosity on particle segregation in a rotating drum. *Powder Technology*, 201(3):266–272, 2010.

[22] H. Al-Hashemi and O. Al-Amoudi. A review on the angle of repose of granular materials. *Powder Technology*, 330:397–417, 2018.

[23] Y. Jin, H. Lu, X. Guo, and X. Gong. Effect of water addition on flow properties of lignite particles. *Chemical Engineering Research and Design*, 132:1020–1029, 2018.

[24] Y. Guo, C. Wassgren, W. Ketterhagen, B. Hancock, and J. Curtis. Discrete element simulation studies of angles of repose and shear flow of wet, flexible fibers. *Soft Matter*, 14(15):2923–2937, 2018.

[25] L. Santos, R. Condotta, and M. Ferreira. Flow properties of coarse and fine sugar powders. *Journal of Food Process Engineering*, 41(2):12648, 2018.

[26] H. Chou, S. Chou, and S. Hsiau. The effects of particle density and interstitial fluid viscosity on the dynamic properties of granular slurries in a rotating drum. *Powder Technology*, 252:42–50, 2014.

[27] C. Liao. A study of the effect of liquid viscosity on density-driven wet granular segregation in a rotating drum. *Powder Technology*, 325:632–638, 2018.

[28] V. Golovanevskiy, V. Arsentyev, I. Blekhman, V. Vasilkov, Y. Azbel, and K. Yakimova. Vibration-induced phenomena in bulk granular materials. *International Journal of Mineral Processing*, 100(3-4):79–85, 2011.

[29] A. Rosato and C. Windows-Yule. Effects of material properties on segregation. In *Segregation in Vibrated Granular Systems*. Academic Press, 2020.

[30] J.M.N.T. Gray. Particle segregation in dense granular flows. *Annual review of fluid mechanics*, 50(1):407–433, 2018.

[31] P. Tahmasebi. A state-of-the-art review of experimental and computational studies of granular materials: properties, advances, challenges, and future directions. *Progress in Materials Science*, page 101157, 2023.

[32] A. Kafaei, S. Akbari, S. Laliberté-Riverin, L. Gosselin, H. Alamdari, and S.M. Taghavi. Time-dependent response of coke-glycerin mixtures to mechanical vibration. In *Proceedings of the 42nd International ICSOBA Conference*, volume 53, pages 989–998. TRAVAUX, 2024.

[33] Y. Zhou, B. Xu, A. Yu, and P. Zulli. An experimental and numerical study of the angle of repose of coarse spheres. *Powder Technology*, 125(1):45–54, 2002.